

Molecular Cancer Therapeutics



Rapamycin Regulates Stearoyl CoA Desaturase 1 Expression in Breast Cancer

David Luyimbazi, Argun Akcakanat, Priscilla F. McAuliffe, et al.

Mol Cancer Ther 2010;9:2770-2784. Published OnlineFirst September 28, 2010.

Updated Version

Access the most recent version of this article at:
doi:[10.1158/1535-7163.MCT-09-0980](https://doi.org/10.1158/1535-7163.MCT-09-0980)

Supplementary Material

Access the most recent supplemental material at:
<http://mct.aacrjournals.org/content/suppl/2010/09/24/1535-7163.MCT-09-0980.DC1.html>

Cited Articles

This article cites 61 articles, 31 of which you can access for free at:
<http://mct.aacrjournals.org/content/9/10/2770.full.html#ref-list-1>

E-mail alerts

[Sign up to receive free email-alerts](#) related to this article or journal.

Reprints and Subscriptions

To order reprints of this article or to subscribe to the journal, contact the AACR Publications Department at pubs@aacr.org.

Permissions

To request permission to re-use all or part of this article, contact the AACR Publications Department at permissions@aacr.org.

Rapamycin Regulates Stearoyl CoA Desaturase 1 Expression in Breast Cancer

David Luyimbazi¹, Argun Akcakanat¹, Priscilla F. McAuliffe¹, Li Zhang², Gopal Singh¹, Ana Maria Gonzalez-Angulo³, Huiqin Chen³, Kim-Anh Do⁴, Yuhuan Zheng¹, Mien-Chie Hung^{5,7}, Gordon B. Mills⁶, and Funda Meric-Bernstam¹

Abstract

Mammalian target of rapamycin (mTOR) signaling is a central regulator of protein translation, cell growth, and metabolism. Alterations of the mTOR signaling pathway are common in cancer, making mTOR a promising therapeutic target. In clinical trials, rapamycin analogs have shown modest response rates for most cancer types, including breast cancer. Therefore, there is an urgent need to better understand the mechanism of action of rapamycin to improve patient selection and to monitor pathway inhibition. To identify novel pharmacodynamic markers of rapamycin activity, we carried out transcriptional profiling of total and polysome-associated RNA in three breast cancer cell lines representing different subtypes. In all three cell lines, we found that rapamycin significantly decreased polysome-associated mRNA for stearoyl-CoA desaturase 1 (SCD1), the rate-limiting enzyme in monounsaturated fatty acid synthesis. Activators of mTOR increased SCD1 protein expression, whereas rapamycin, LY294002, and BEZ235 decreased SCD1 protein expression. Rapamycin decreased total SCD1 RNA expression without inducing a significant decline in its relative polysomal recruitment (polysome/total ratio). Rapamycin did not alter SCD1 mRNA stability. Instead, rapamycin inhibited *SCD1* promoter activity and decreased expression of mature transcription factor sterol regulatory element binding protein 1 (SREBP1). Eukaryotic initiation factor 4E (eIF4E) small interfering RNA (siRNA) decreased both SCD1 and SREBP1 expression, suggesting that SCD1 may be regulated through the mTOR/eIF4E-binding protein 1 axis. Furthermore, SCD1 siRNA knockdown inhibited breast cancer cell growth, whereas overexpression increased growth. Taken together these findings show that rapamycin decreases SCD1 expression, establishing an important link between cell signaling and cancer cell fatty acid synthesis and growth. *Mol Cancer Ther*; 9(10); 2770–84. ©2010 AACR.

Introduction

Mammalian target of rapamycin (mTOR) regulates cell growth and metabolism. Its best studied targets are eukaryotic initiation factor 4E (eIF4E)-binding protein 1 (4E-BP1), which regulates the availability of eIF4E, a rate limiting factor for cap-dependent translation, and S6 kinase 1 (S6K1), which regulates ribosomal S6 phosphorylation. Rapamycin is a macrolide fungicide that inhibits mTOR signaling by binding to FK506-binding protein

12 (1). Although many breast cancer cell lines are sensitive to the growth-inhibitory effects of rapamycin in preclinical models (2–4), the overall response rates observed in clinical studies involving mTOR inhibitors in patients with breast cancer have been modest (5–7). These findings have prompted further studies of the mechanism behind the growth-inhibitory effects of rapamycin with the goal of developing effective rational combinatorial therapies.

Cancer cells have increased metabolic autonomy. Compared with normal tissues, cancer cells take up nutrients and metabolize them at high rates to support rapid growth and proliferation. How cancer cells achieve high rates of fatty acid synthesis, and how oncogenic pathways influence this, is not well understood. Stearoyl-CoA desaturase 1 (SCD1) is a critical mediator of fatty acid synthesis. SCD1 catalyzes the introduction of the first double bond in the *cis*- Δ^9 position of saturated fatty acyl-CoAs, such as palmitoyl- and stearoyl-CoA. This rate-determining step produces monounsaturated fatty acids, namely palmitoleoyl- and oleoyl-CoA (8), which in turn provide substrates for the development of polyunsaturated fatty acids. SCD1 therefore has a direct effect on the ratio of saturated to monounsaturated fatty acids. An unbalanced ratio contributes to altered membrane

Authors' Affiliations: Departments of ¹Surgical Oncology, ²Bioinformatics and Computational Biology, ³Breast Medical Oncology, ⁴Biostatistics, ⁵Molecular and Cellular Oncology, and ⁶Systems Biology, The University of Texas M.D. Anderson Cancer Center, Houston, Texas; and ⁷Center for Molecular Medicine and Graduate Institute of Cancer Biology, China Medical University and Hospital, Taichung, Taiwan

Note: Supplementary material for this article is available at Molecular Cancer Therapeutics Online (<http://mct.aacrjournals.org/>).

Corresponding Author: Funda Meric-Bernstam, 1400 Holcombe Boulevard, Unit 444, Houston, TX 77030. Phone: 713-745-4453; Fax: 713-745-4926. E-mail: fmeric@mdanderson.org

doi: 10.1158/1535-7163.MCT-09-0980

©2010 American Association for Cancer Research.

fluidity and has been implicated in a variety of diseases, including cancer (9, 10). Further, the activity of a number of lysophospholipid growth factors such as lysophosphatidic acid, which is implicated in the development and progression of breast cancer, is altered by the saturation of fatty acyl chains (11). Lipid analyses from transformed cell lines have indicated an increase in the conversion of saturated stearic acid to monounsaturated oleic acid, reflecting a significant decrease in the saturation index of the cell (12, 13). SCD1 is overexpressed in mouse models genetically susceptible to hepatocarcinogenesis, suggesting that SCD1 may play a role in carcinogenesis (14, 15). Further, SCD1 has recently been identified in a RNA interference screen as a potential target for cancer therapy (16). Thus, further work is needed to determine the regulators of fatty metabolism and specifically SCD1 in cancer cells.

The role of mTOR in metabolism is shown by its ability to integrate nutrient availability and energy through amino acid biosynthesis and glucose homeostasis (17). Recent studies have also pointed to a role for mTOR in adipogenesis (18–20). Clarifying the role of mTOR in cellular fat metabolism is important in understanding how tumor cells support the accelerated metabolism essential for increased cell proliferation.

To identify novel pharmacodynamic markers of response to rapamycin as well as potential targets for combinatorial therapy, we carried out a high-throughput microarray polysome analysis of three rapamycin-sensitive breast cancer cell lines representing the key breast cancer subtypes to identify genes regulated at the transcriptional or translational level. We show here that rapamycin causes a dramatic decrease in SCD1 mRNA and protein expression. Rapamycin inhibits *SCD1* promoter activity, and it decreases expression of mature sterol regulatory element binding protein 1 (SREBP1), a transcription factor involved in fatty acid and cholesterol homeostasis (21). We also show that SCD1 is regulated by eIF4E, suggesting mTOR may regulate SCD1 through the mTOR/4E-BP1/eIF4E axis. Furthermore, suppression of SCD1 inhibits breast cancer cell growth, whereas overexpression increases cell growth. These findings support an important link between the oncogenic cell signaling of mTOR and cancer cell fat metabolism. This novel observation is important in understanding how tumor cells establish and support the accelerated fatty acid synthesis essential for increased cell proliferation.

Materials and Methods

Cell lines and cultures

BT-20, BT-474, BT-483, BT-549, HCC1143, HCC1937, MCF7, MDA-MB-157, MDA-MB-231, MDA-MB-361, MDA-MB-436, MDA-MB-468, SK-Br-3, T47D, and ZR-75-1 cells were obtained from the American Type Tissue Culture Collection (ATCC) in January 2006. Cell lines were passaged for <6 months after resuscitation, and thus were not tested for characterization. The ATCC Molecular Authentication Resource Center provides a varie-

ty of applications to identify and characterize the cell lines, including cloning and gene synthesis, real-time PCR analyses, site-directed mutagenesis, sequencing, short tandem repeat, single nucleotide polymorphism, and fingerprint analyses (<http://www.atcc.org/Science/AuthenticationandPreservation/AuthenticationTechnology/tabid/209/Default.aspx>). Cells were cultured in DMEM/F12 supplemented with 10% fetal bovine serum at 37°C and humidified 5% CO₂. Lipoprotein-deficient serum was purchased from Sigma-Aldrich. Stable SCD1-overexpressing cell lines and controls were generated using MDA-MB-231 cells transfected with either myc/DDK-tagged human SCD1 ORF DNA clone or its control vector. Colonies were then selected with G418 at a final concentration of 2 mg/mL, and positive colonies were confirmed by Western blot analysis.

Reagents

Rapamycin, LY294002, and cyclohexamide were purchased from LC Laboratories, Inc. DMSO, insulin-like growth factor-I (IGF-I), insulin, actinomycin D, and mevlinol were purchased from Sigma-Aldrich. BEZ235 was kindly provided by Novartis Institutes for Biomedical Research-Novartis Oncology. Chemical structures of rapamycin (22), LY294002 (23), and BEZ235 (24) are shown in Supplementary Fig. S1.

Oligonucleotides and plasmids

Oligonucleotides were synthesized by Sigma-Aldrich. The human SCD1 cDNA, the human β -actin cDNA, and the myc/DDK-tagged human SCD1 ORF and its control were all obtained from Origene Technologies, Inc. The promoter-reporter gene plasmid hSCD-Luc pGL3 was a gift from Dr. James M. Ntambi (University of Wisconsin, Madison, WI; ref. 25). The pRL-TK vector was obtained from Promega Corporation. Constitutively active (CA) Akt plasmid was provided by Dr. Philip N. Tsichlis (Fox Chase Cancer Center, Philadelphia, PA). 4E-BP1 wild-type (4E-BP1 WT) and 4E-BP1 five phosphorylation sites mutated (4E-BP1 5A) plasmids were provided by Dr. Thurl E. Harris (University of Virginia, Charlottesville, VA).

Sucrose density gradients

After cells were treated with either rapamycin or control for 24 hours, sucrose density gradients were done as described elsewhere (26). The resulting monosomal and polysomal fractions were pooled and RNA was extracted.

RNA extraction for microarray analysis

Both monosomal and polysomal RNA were extracted by phenol and chloroform. Total RNA from all *in vitro* samples was extracted using TRIzol reagent per the manufacturer's protocol (Invitrogen). Total RNA from xenografts was extracted using the RNeasy Mini Kit (Qiagen Inc.). Total and polysomal RNA were hybridized to Affymetrix Human Genome U133 Plus 2.0 chips (Affymetrix, Inc.).

Real-time PCR analysis

Real-time PCR was done on the ABI PRISM 7900HT Sequence Detection System (Applied Biosystems). The Assays-on-Demand gene expression products used included human *SCD1* (Hs01682761m1), 18S (4319413E), *β-actin* (4326315E), and glyceraldehyde 3-phosphate dehydrogenase (*GAPDH*; 4326317E; Applied Biosystems). TaqMan Universal PCR Master Mix (Applied Biosystems) was used to amplify the cDNA. The Sequence Detection System software automatically determined fold-change for *SCD1* in each sample relative to the endogenous control.

Western blot analysis

Cells were washed with cold PBS and lysed in either 100 mmol/L Tris-HCl (pH 6.8), 4% SDS, and 20% glycerol, or 1% Triton X-100, 150 mmol/L NaCl, 20 mmol/L sodium phosphate buffer (pH 7.4), 1% aprotinin, 5 mmol/L phenylmethylsulfonyl fluoride, 10 μg/mL leupeptin, 100 mmol/L NaF, 2 mmol/L Na₃VO₄, 1 mmol/L EGTA, and 5 mmol/L sodium pyrophosphate. Cell lysates containing 50 μg of protein were separated by SDS-PAGE. The protein was transferred to a 0.2 μmol/L polyvidine difluoride membrane (Bio-Rad Laboratories). Membranes were blocked in 0.1% casein in TBS.

The *SCD1* antibodies were from Santa Cruz Biotechnology, Inc. Antibodies against total Acetyl CoA Carboxylase (ACC), total Akt, phospho-Akt (Thr 308), phospho-Akt (Ser 473), mTOR, total S6K1, phospho-S6K1 (Thr 389), eIF4E, and phospho-S6 ribosomal protein (S6RP; Ser 240/244) were purchased from Cell Signaling Technology, Inc. Antibodies against fatty acid synthase (FAS) and SREBP1 were purchased from BD Biosciences, Inc. Antibodies against *β-actin* were from Sigma-Aldrich. The immunoblots were visualized using either the Odyssey IR imaging system or software (Li-Cor Biosciences), or the enhanced chemiluminescence detection kit (ECL) from GE Healthcare Corp.

Northern blot analysis

Electrophoresis of total RNA and Northern analysis were done using the NorthernMax kit (Ambion Inc.). The *SCD1* probe was constructed via PCR reaction from a plasmid containing the human *SCD1* cDNA clone using 5'-CCACAGCATATCGCAAGAAA-3' as the forward primer and 5'-CCCAGCTGTCAAAGAGAAGG-3' as the reverse primer. The *β-actin* probe was constructed similarly, from a plasmid containing the human *β-actin* cDNA clone using 5'-GGCATCTCACCCCTGAAGTA-3' as the forward primer and 5'-GGGGTGTGAAGGTC-CAAA-3' as the reverse primer. The respective probes were labeled with α P32 dCTP using the Prime-a-Gene Labeling System (Promega). Unincorporated radioisotope was removed using Illustra MicroSpin G-25 columns (GE Healthcare Corp.). All blots were developed using a Molecular Dynamics Storm 860 phosphorimager (GE Healthcare Corp.).

Small interfering RNA

The silencing of *SCD1*, mTOR, S6K1, or eIF4E with small interfering RNA (siRNA) was achieved by using DharmaFECT 1 transfection reagent (Dharmacon, Inc.). The mTOR single siRNA sequence was CCCUGCCUUU-GUCAUGCCU (27). The eIF4E single siRNA sequence 1 was GGAUGGUAUUGAGCCUAUG and sequence 2 was GCAAACCUGCGGCUGAUCU (28). The S6K1 single siRNA sequence 1 was CAGUGGAGGAGAA-CUAUUU (29), sequence 2 was CUUCUGGCUCGAA-GGUGG, and sequence 3 was UGUAUGACAUGCUGACUGG. The S6K1 pool sequences were CAUGGAA-CAUUGUGAGAAAUU, GGAAUGGGCAUAAGUU-GUAUU, GUAAAUGGCUUGUGAUACUUU, and CAAAUUAGCAUGCAAGCUUUU (29). The *SCD1* single siRNA sequence was CUACGGCUCUUUCUGAU-CAUU and sequence 2 was GAGAUAGUUGGAGAC-GAUUU (16). The *SCD1* pool siRNA sequences were CUACAAGAGUGGCUGAGUUUU, CUACGGCUCUUUCUGAUCAUU, GCACAACAACUUCACCA-CAUU, and GAACAGUGCUGCCCACCUCUU (Dharmacon). A negative control single siRNA was used for experiments involving single sequence siRNA, and pool siRNA sequences were used in the silencing of *SCD1*. All siRNAs were purchased from Dharmacon, Ambion, or Sigma.

RNA stability study

MDA-MB-468 cells were inoculated with either rapamycin or vehicle at 12 time points spanning 24 hours. All samples were incubated with actinomycin D at a final concentration of 5 μg/mL. No treatment was given at the 0 hour time points, which were the designated controls for each study. Total RNA was extracted with TRIzol and analyzed via Northern blotting.

Transient transfection and dual reporter gene assay

Transient cotransfections were done using the FuGENE 6 transfection reagent per manufacturer's protocol (Roche Applied Science, Inc.). Each experiment was done in triplicate. For rapamycin regulation of *SCD1* experiments, cells were transfected with 0.5 μg/well of both h*SCD*-Luc pGL3 and pRL-TK plasmids. Transfected cells were incubated in complete medium for 24 hours, followed by serum-free medium 12 hours prior to treatment. The cells were then treated in 100 nmol/L rapamycin, 5 μmol/L mevinolin, or a combination in media with 10% lipid-deficient serum. Cells were harvested 24 hours after treatments using the Dual Luciferase Reporter Assay System (Promega). For 4E-BP1 plasmid cotransfection experiments, cells were transfected with 1 μg/well of h*SCD*-Luc pGL3, pRL-TK, and empty vector, or 4E-BP1 WT or 4E-BP1 5A plasmids. Transfected cells were incubated in complete medium for 72 hours, followed by a combination media with 10% lipid-deficient serum. Cells were harvested 24 hours after treatments using the Dual Luciferase Reporter Assay System (Promega). All readings were

done using a Sirius Single Tube Luminometer (Berthold Detection Systems).

In vivo studies

All animal studies were approved by the M.D. Anderson Animal Care and Use Committee. The animal care program is fully accredited by the Association for the Assessment and Accreditation of Laboratory Animal Care, International. Eight-week-old female *nu/nu* mice (Harlan Sprague Dawley Inc.) were inoculated with 1.5×10^7 MDA-MB-468 or MCF7 cells in their mammary fat pads. After 75 to 150 mm³ tumors formed, mice were given weekly i.p. injections of either rapamycin (15 mg/kg) or DMSO for 3 weeks. Mice were euthanized 24 hours after the first or fourth weekly injection. Tumors were harvested, and RNA was extracted using RNeasy (Qiagen).

Reverse phase proteomic array

Protein lysates were prepared from frozen mice xenografts and printed on nitrocellulose-coated slides. Slides were probed with phospho-S6 ribosomal protein (Ser 240/244) antibody (Cell Signaling Technology), which was validated for reverse phase proteomic array (RPPA). The detailed procedure is described elsewhere (30).

SREBP1 transcription factor assay

Nuclear protein was extracted using a Nuclear/Cytosol Fractionation Kit (BioVision Inc.). Specific transcription factor DNA binding activity was then assayed using a human SREBP1 Transcription Factor Assay Kit (Cayman Chemical Co.).

Cell growth, dose-effect, and cell cycle analysis

Cell growth was determined by the protein content of treated and untreated cells through the sulforhodamine B (SRB) assay (31). The experiment was done in 96-well plates in triplicate. Plated cell numbers were adjusted according to the growth rate of the cell lines. Absorbance was measured at a wavelength of 570 nm. Dose-effect and IC₅₀ analysis are described elsewhere (32). Cell cycle analysis was done as previously described (33).

Statistical analysis

All results formatted as bar graphs are presented as means \pm SE. Data were analyzed using Student's *t*-test, one-way ANOVA, and Spearman rank correlation tests where appropriate by GraphPad Prism v5.01 software (GraphPad Software).

The probe intensities on microarrays were processed using the Position-Dependent Nearest Neighbor model to estimate gene expression values (34). The β Uniform mixture model (35) was used to estimate false discovery. The gene list was considered significant at a false discovery rate of 20%. For all other analyses, differences were considered significant at $P < 0.05$. Two group comparisons were done by using Student's *t*-test using the false discovery rate cutoff of 20% for both total and polysomal RNA groups, and the data are presented as

mean \pm SE. Calculations and presentations of microarray data were done in log 2. Calculations of RPPA data were done in log 2.

Results

Rapamycin treatment suppresses SCD1 expression *in vitro*

We sought to identify genes regulated by rapamycin in three cell lines representing different breast cancer subtypes: MDA-MB-468, estrogen receptor/progesterone receptor/human epidermal growth factor receptor 2 (HER2) negative, i.e., triple negative; MCF7, estrogen receptor positive; and BT-474, HER2 positive. As rapamycin has been shown to affect transcription and translation (36, 37), we compared the gene expression profiles of total cellular mRNA and polysome-associated, translationally active mRNA in the presence and absence of rapamycin (Fig. 1A). Cells were treated with 100 nmol/L rapamycin, a dose that significantly inhibits growth in all three breast cancer cell lines and that has been shown to be a clinically achievable peak concentration in temsirolimus trials (38, 39). In all three cell lines, we found a statistically significant drop in the levels of polysome-associated mRNA for SCD1, suggesting that there is a decline in translationally active SCD1 mRNA in all three cell lines. There was a 2.8-fold decline in MDA-MB-468 cells ($P = 0.010$), a 2.1-fold decline in MCF7 cells ($P = 0.001$), and a 5.7-fold decline in BT-474 cells ($P = 0.002$) after rapamycin treatment. SCD1 total RNA levels in MDA-MB-468 cells declined by 2.3-fold after rapamycin treatment ($P = 0.026$), raising the possibility that the decline in polysomal mRNA could be due to a decrease in total RNA. In MCF7 cells, there was a minimal drop in total SCD1 mRNA levels upon rapamycin treatment by microarray analysis, and although there was a decline in total RNA in BT-474 cells ($P = 0.011$), this was not statistically significant using a false discovery rate cutoff of 20%. Thus, in MCF7 and BT-474 cells we could not determine by microarray analysis whether the drop in polysomal SCD1 levels was primarily attributable to a decrease in total RNA or a decrease in polysomal recruitment of SCD1 mRNA.

To evaluate the mechanism of SCD1 downregulation by rapamycin, we used quantitative reverse transcriptase-PCR (Q-PCR) to assess SCD1 mRNA levels in total RNA, and monosomal and polysomal RNA fractions in MDA-MB-468 and MCF7 cells cultured in the absence or presence of rapamycin. Total RNA was isolated after 24 hours of exposure to either 100 nmol/L rapamycin or vehicle. Cell lysates were separated with sucrose gradient centrifugation to obtain pooled monosomal and polysomal RNA batches. Real-time PCR was done to quantitate relative RNA levels for SCD1 and actin in both total RNA and the monosomal and polysomal fractions. The results were similar to those observed by microarray analysis, but on Q-PCR a statistically significant decline in total SCD1 mRNA was shown in both MDA-MB-468 and MCF7 cells. Q-PCR revealed a significant decrease in

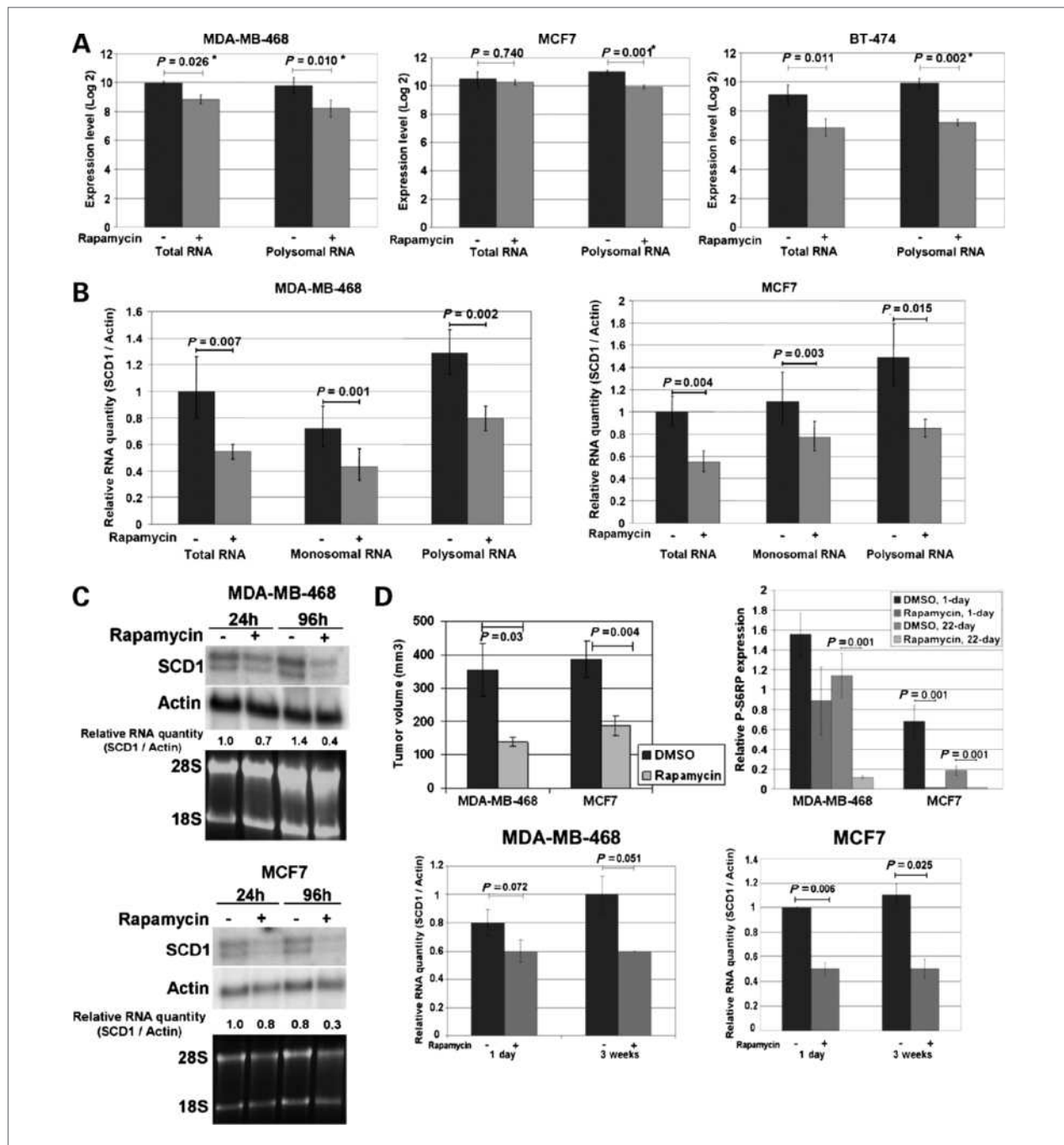


Figure 1. Rapamycin decreases SCD1 expression. **A**, MDA-MB-468, MCF7, and BT-474 cells were treated with 100 nmol/L rapamycin or 0.01% DMSO for 24 hours. Polysomal RNA was separated by sucrose gradient centrifugation. Total polysomal RNA was extracted and hybridized to Affymetrix Human Genome U133 Plus 2.0 chips. The RNA expression in the rapamycin-treated samples was compared with that of untreated total and polysomal RNA samples using Student's *t*-test. The gene of interest was considered significant in each cell line if it met a false discovery rate of 20%. All comparisons that met this cutoff are demarcated by an asterisk (*). Data are means \pm SE. **B**, Q-PCR analysis was done to quantitatively assess total RNA, and monosomal and polysomal fractions in MDA-MB-468 and MCF7 cells treated with rapamycin versus vehicle for 24 hours. Actin was used as the endogenous control. RNA expression in rapamycin-treated and untreated samples was compared by using Student's *t*-test. Data are means \pm range (min-max). **C**, Northern blot analysis for SCD1 and actin was done on total RNA isolated from MDA-MB-468 and MCF7 cells grown in either rapamycin or vehicle for 24 and 96 hours. **D**, to study the effect of rapamycin on SCD1 *in vivo*, MDA-MB-468 or MCF7 xenografts were treated with either rapamycin or vehicle for 1 day or 3 weeks. Tumor volumes at day 22 are shown as means \pm SE. Vehicle versus rapamycin groups were compared using Student's *t*-test (top left). Protein lysates prepared from three xenografts were printed on RPPA slides and probed with P-S6RP (Ser 240/244) antibody. Relative P-S6RP expression in rapamycin-treated and untreated groups were compared by using Student's *t*-test (top right). Data are means \pm SE. Total RNA from three tumor samples from each group was evaluated using Q-PCR to assess SCD1 and actin expression (bottom). Data are means \pm SE.

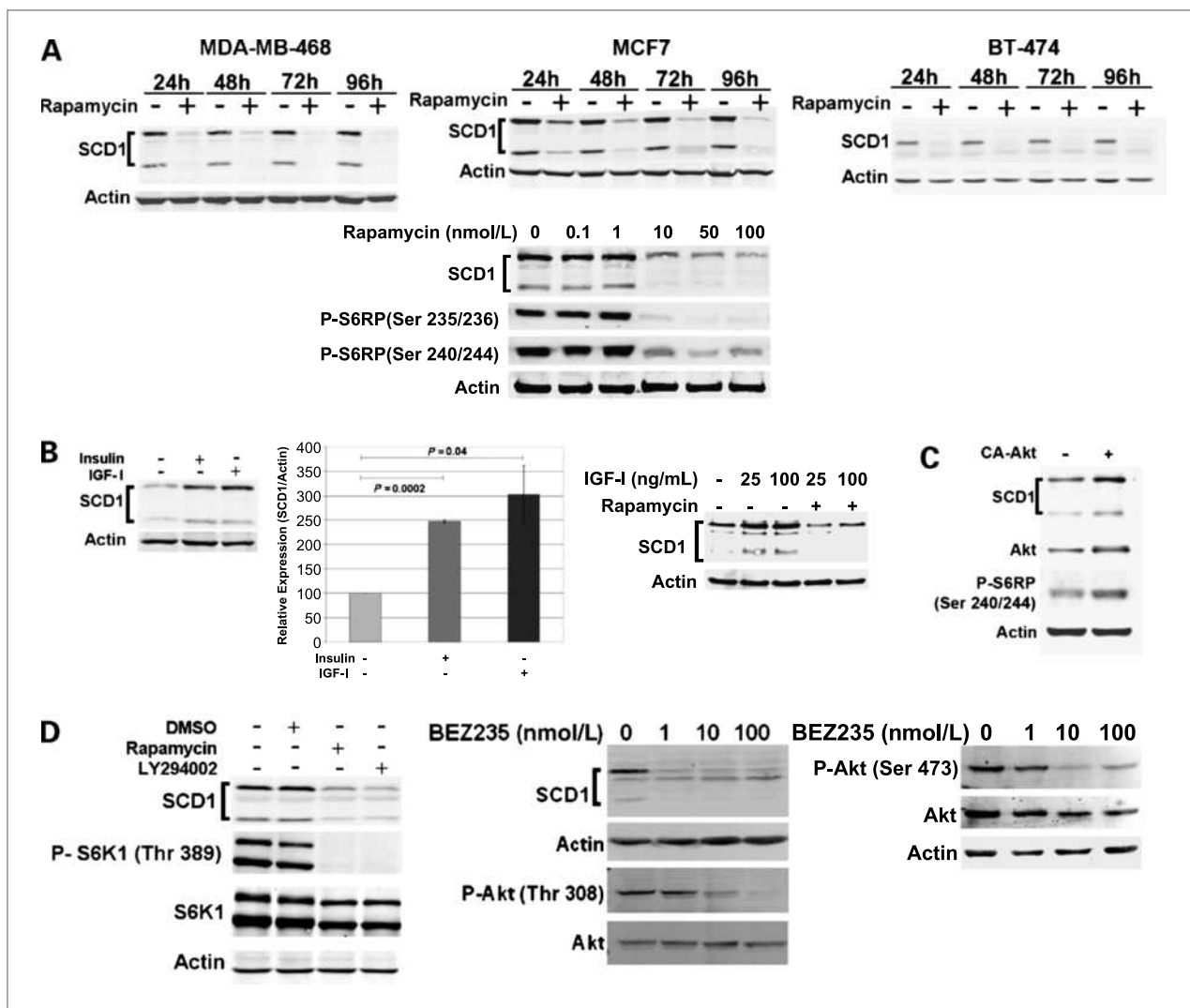


Figure 2. SCD1 expression is inhibited by PI3K/mTOR inhibitors and increased by insulin signaling. **A**, MDA-MB-468, MCF7, and BT-474 cells were treated with 100 nmol/L rapamycin or DMSO for 24, 48, 72, and 96 hours, and 10% SDS-PAGE and Western blotting using SCD1 and actin antibody were done (top). MCF7 cells were treated with various concentrations of rapamycin for 96 hours. Western blotting was done using SCD1 and actin antibody (bottom). **B**, MCF7 cells were incubated overnight in serum-free media. Cells were then cultured for 8 hours in one of the following conditions: no treatment, medium containing 10 μ g/mL of insulin, or 100 ng/mL of IGF-I. SDS-PAGE (10%) and Western blotting using SCD1 antibody and actin were done (left). The experiments were replicated in triplicate and quantified according to a relative expression of SCD1/ β -actin. Top band was used for quantification. Relative SCD1 expression in the treatment groups was compared with that of the no treatment group using Student's *t*-test (middle). Data are means \pm SE. After overnight serum starvation, cells were cultured for 8 hours in one of the following conditions: no treatment or medium containing 25 or 100 ng/mL of IGF-I in the absence or presence of pretreatment with 100 nmol/L rapamycin (right). SDS-PAGE (10%) and Western blotting using SCD1 antibody and actin were done. **C**, MCF7 cells were transfected with control and constitutively active Akt (CA-Akt) plasmids. Sixty hours later, serum-free media were added and cells were incubated for an additional 36 hours. Western blotting was done for SCD1, Akt, P-S6RP (Ser 240/244), and actin (right). **D**, left, MDA-MB-468 cells were cultured for 24 hours with no treatment, DMSO, 100 nmol/L rapamycin, and 50 μ mol/L LY294002. Western blotting was done using SCD1 and actin antibody. S6K1 and phospho-S6K1 (Thr 389) were used to confirm inhibition of the mTOR pathway. Middle, MDA-MB-468 cells were cultured with DMSO, or 1, 10, or 100 nmol/L BEZ235. Lysates were collected at 6 hours (for P-Akt and Akt) or 24 hours (for SCD1 and actin). Western blotting was done using P-Akt (Thr 308), Akt, SCD1, and actin antibody. Right, MDA-MB-468 cells were cultured with DMSO or 1, 10, or 100 nmol/L BEZ235. Lysates were collected at 6 hours and Western blotting was done using P-Akt (Ser 473), Akt, and actin antibody.

SCD1 mRNA in both the monosomal and the polysomal RNA fractions exposed to rapamycin compared with vehicle (Fig. 1B). Similar results were obtained when SCD1 was normalized to GAPDH or 18S ribosomal RNA (data not shown). These results argue against the regulation of SCD1 by rapamycin at the translational level, as transla-

tional regulation would have led to a drop in polysomal fractions and an increase in monosomal fractions. Instead, the decline in total SCD1 mRNA as well as mRNA in both polysomal and monosomal fractions suggests that the regulation of SCD1 by rapamycin occurs primarily at the level of total RNA.

To confirm this observation, total RNA from both cell lines was isolated after 24 or 96 hours of exposure to rapamycin or vehicle, and Northern analysis was done (Fig. 1C). The data reveal two transcripts (3.0 and 5.2 kb) that are known to encode the same size polypeptide (40). Rapamycin treatment was associated with a >50% reduction in SCD1 mRNA levels. Both transcripts were equally repressed in the presence of rapamycin. These findings confirm the regulation of total SCD1 RNA by rapamycin.

Rapamycin treatment decreases growth and suppresses SCD1 expression *in vivo*

To determine the effect of rapamycin on tumor growth and SCD1 expression *in vivo*, we inoculated mice with MDA-MB-468 or MCF7 cells and once tumors had formed treated the mice with rapamycin or vehicle for 1 day or 3 weeks. Xenografts of both cell lines showed

statistically significant inhibition of tumor growth with rapamycin treatment. Tumor volumes of MDA-MB-468 xenografts on day 22 were $355 \pm 80 \text{ mm}^3$ (mean \pm SE) in the DMSO group and $140 \pm 13 \text{ mm}^3$ in the rapamycin-treated group ($P = 0.03$). Tumor volumes of MCF7 xenografts on day 22 were $388 \pm 54 \text{ mm}^3$ in the DMSO group and $187 \pm 29 \text{ mm}^3$ in the rapamycin group ($P = 0.004$) (Fig. 1D). Next, we assessed the effect of rapamycin on mTOR downstream signaling by RPPA in xenografts treated with rapamycin for 1 day, or weekly for 3 weeks; tumors were in both cases harvested approximately 24 hours after rapamycin treatment. After 3 weeks of treatment, rapamycin significantly reduced P-S6RP (Ser 240/244) phosphorylation in MDA-MB-468 xenografts by 90% ($P < 0.001$) and in MCF7 xenografts by 91% ($P < 0.001$; Fig. 1D). Then we established the effect of rapamycin on SCD1 RNA *in vivo*. SCD1 RNA levels

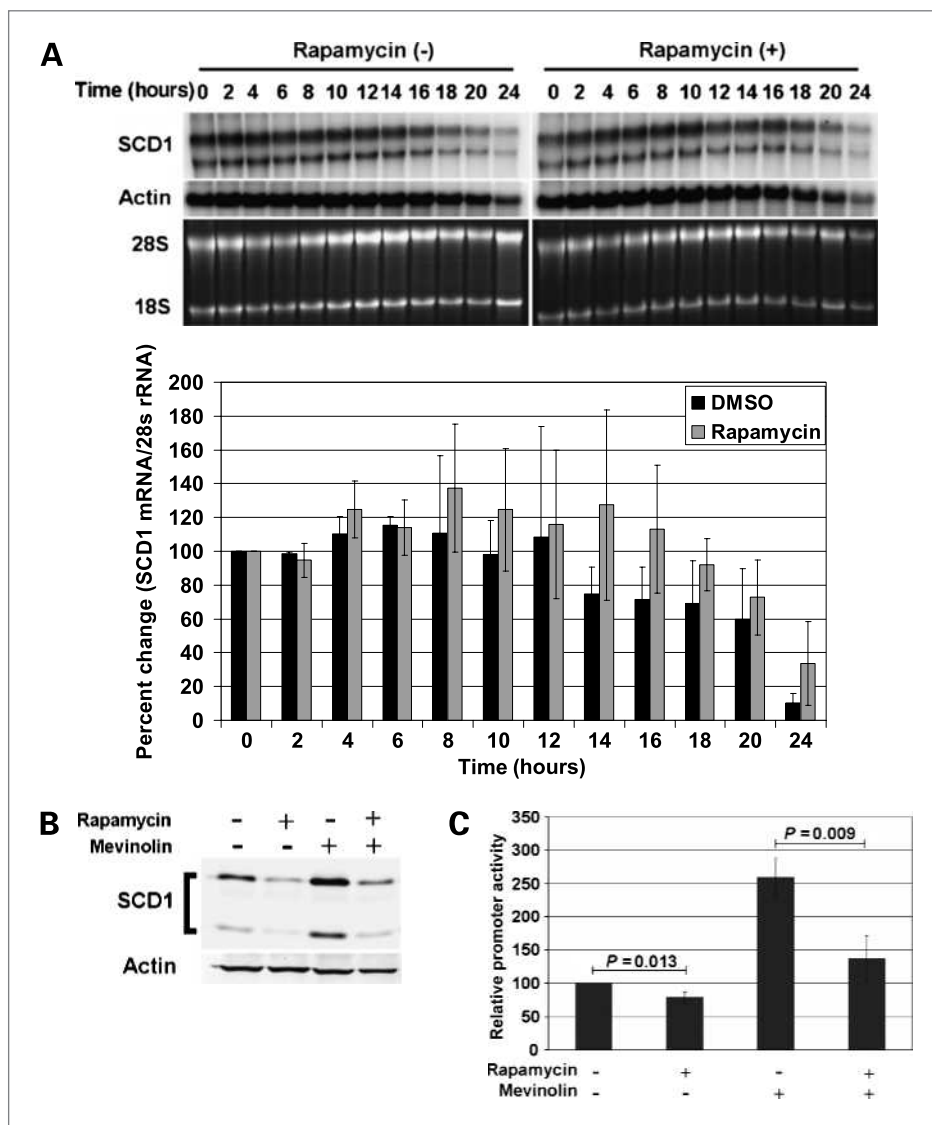


Figure 3. Rapamycin regulates SCD1 promoter activity, but not SCD1 mRNA stability. **A**, MDA-MB-468 cells were treated with 100 nmol/L rapamycin or vehicle at 12 time points spanning 24 hours. All samples were incubated with actinomycin D at a final concentration of 5 $\mu\text{g}/\text{mL}$. No treatment was used at the 0 hour time points, which were the designated controls for each study. Total RNA was extracted from each sample and analyzed via Northern blotting. Quantitation of the Northern blot was shown below. **B**, Western blot analyses in MCF7 cells were used to study the effects of rapamycin (100 nmol/L) on the mevinolin-based (5 $\mu\text{mol}/\text{L}$) induction of SCD1 in medium supplemented with lipid-deficient serum. These results were replicated in triplicate. **C**, dual luciferase assays were done after cotransfecting MCF7 cells with SCD1 promoter reporter (hSCD1-Luc pGL3) and control (pRL) plasmids. Results from triplicate experiments show a repression of the SCD1 promoter by rapamycin.

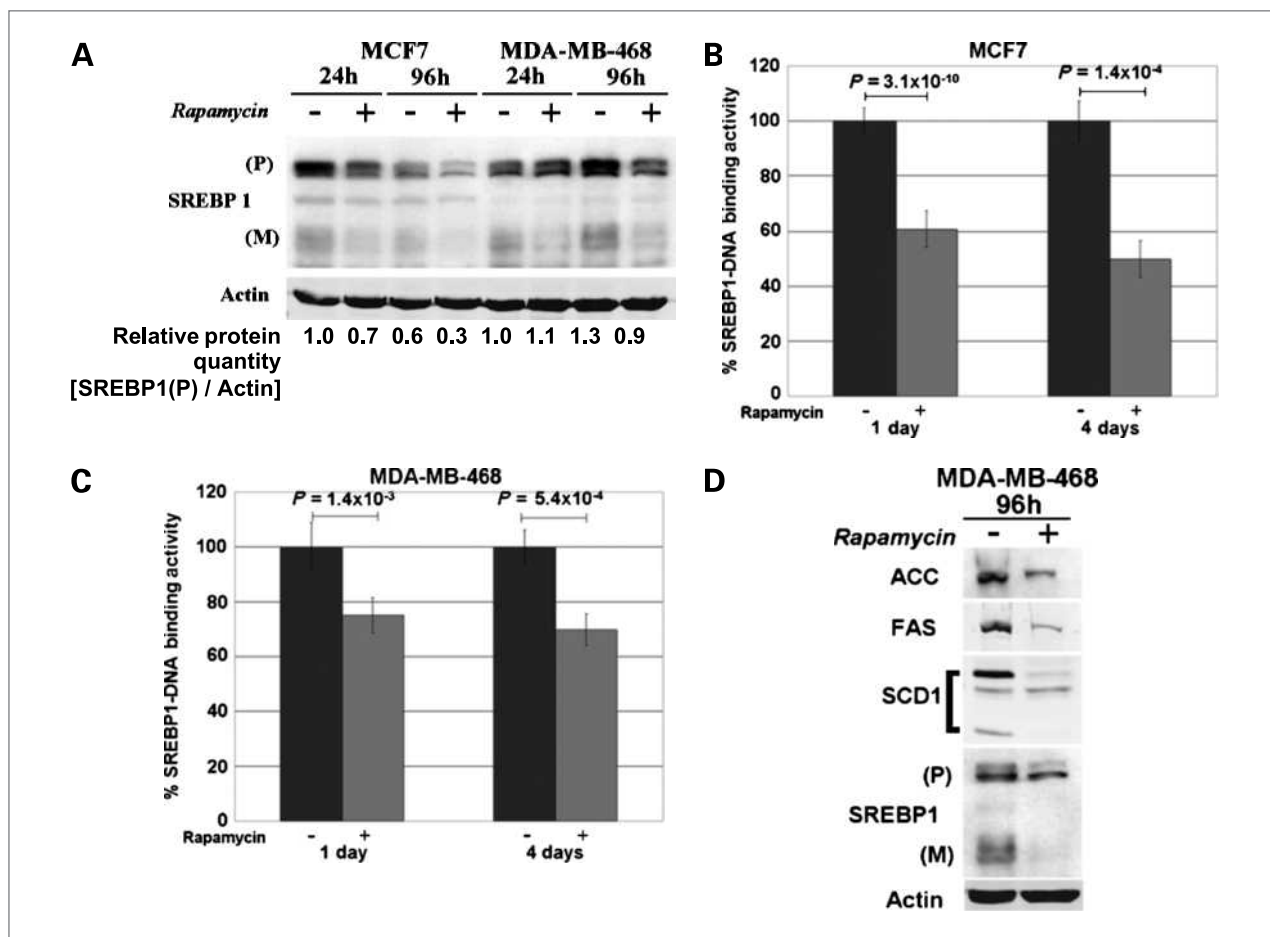


Figure 4. Rapamycin regulates expression of mature SREBP1. A, MCF7 and MDA-MB-468 cells were treated with 100 nmol/L rapamycin or vehicle for 24 and 96 hours. SDS-PAGE (8%) and Western blotting using SREBP1 and actin antibodies were done. Each SREBP1 blot had a precursor band (P) and a smaller mature band (M). These results were confirmed in triplicate experiments. Nuclear protein extracts from MCF7 (B) and MDA-MB-468 (C) cells treated with 100 nmol/L rapamycin or vehicle for 1 and 4 days were assayed for specific transcription factor-DNA binding activity. All experiments were replicated in triplicate and quantified in comparison with vehicle using Student's *t*-test. Data are means \pm SE. D, MDA-MB-468 cells were treated with 100 nmol/L rapamycin for 96 hours. SDS-PAGE and Western blotting using ACC, FAS, SCD1, SREBP1, and actin antibodies were done.

showed some decline in MDA-MB-468 tumors with the change at 3 weeks approaching statistical significance ($P = 0.051$; Fig. 1D). MCF7 tumors showed a significant decline in SCD1 RNA levels at both day 1 and week 3 ($P = 0.006$ and $P = 0.025$, respectively; Fig. 1D). These results show that rapamycin regulates SCD1 total RNA expression both *in vivo* and *in vitro*.

SCD1 expression is increased with activation of PI3K/Akt/mTOR signaling

We sought to determine whether rapamycin regulates SCD1 protein expression. After exposing the cells to rapamycin for 24 to 96 hours, we observed a robust downregulation of SCD1 protein levels in all three cell lines (Fig. 2A). A dominant band and a smaller fragment were noted in most Western blots; the smaller fragment showed equal modulation by rapamycin. This fragment may represent a SCD1 cleavage product (41).

We incubated MCF7 cells with increasing concentrations of rapamycin for 24 hours and found a dose-dependent decrease in SCD1 expression, which became evident at 10 nmol/L (Fig. 2A).

To investigate the role of phosphoinositide 3-kinase (PI3K)/Akt/mTOR signaling in SCD1 expression, we studied the effects of insulin and IGF-I, two mitogens known to induce mTOR activity (42, 43). After 12 hours of serum starvation, MCF7 cells were exposed to either insulin or IGF-I, and their SCD1 expression was compared with cells grown in no serum. Western blot analyses showed an increase in SCD1 expression with both stimuli (Fig. 2B, left). The results from three independent experiments showed that, indeed, both insulin and IGF-I significantly increased SCD1 expression ($P = 0.0002$ and $P = 0.04$, respectively; Fig. 2B, middle). Rapamycin pretreatment was at least in part able to overcome IGF-induced SCD1 overexpression (Fig. 2B,

right). We conducted a gain-of-function experiment and transfected the MCF7 cell line with control and constitutively active Akt plasmids. Sixty hours after transfection, serum was removed and cells were

starved for 36 hours. There was an increase in phosphorylation of S6 ribosomal protein, a downstream target of mTOR, and accompanying increase in expression of SCD1 (Fig. 2C).

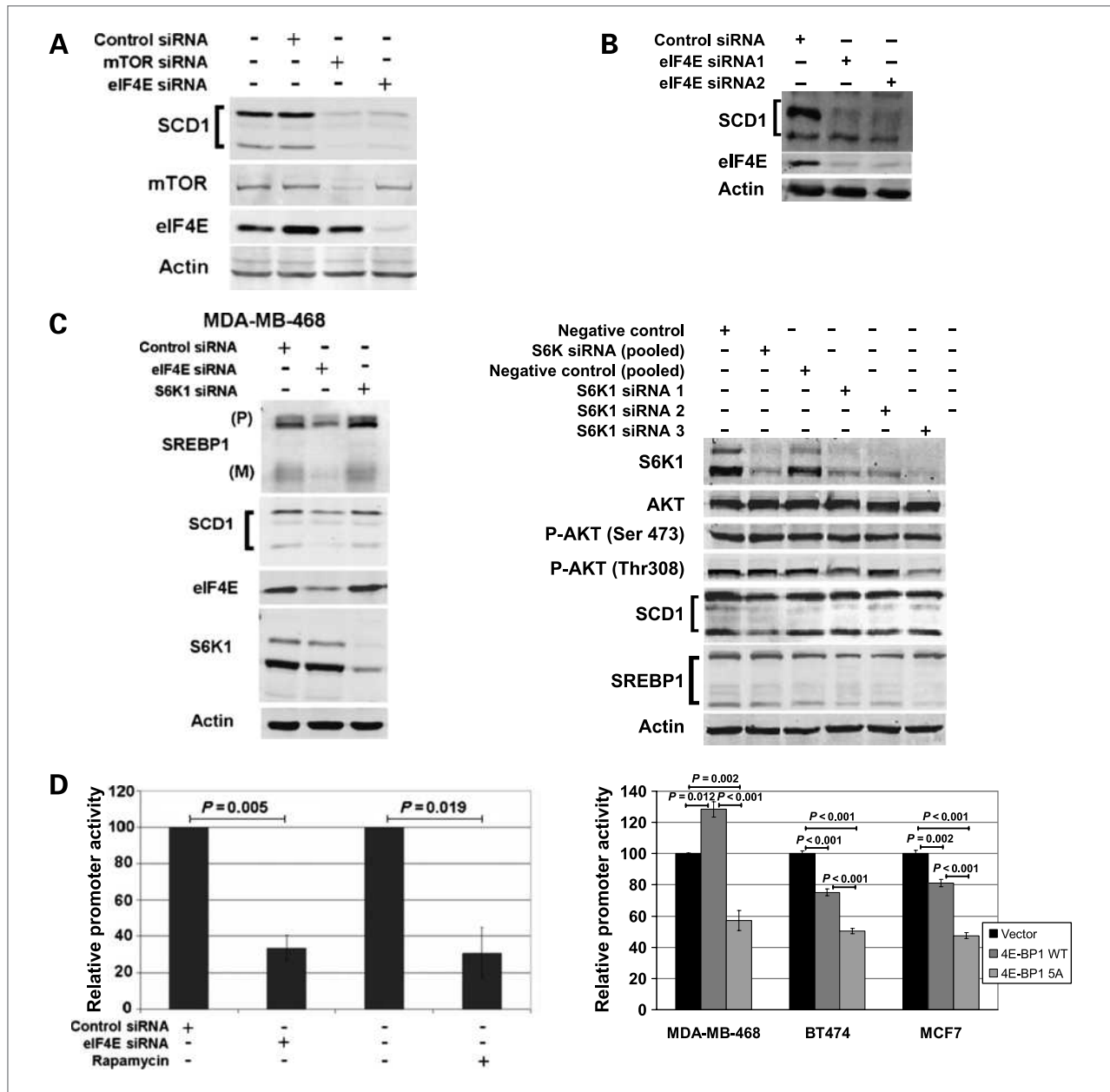


Figure 5. eIF4E knockdown decreases SCD1 and SREBP1 expression and SCD1 promoter activity. **A**, MDA-MB-468 cells were transfected with siRNA for mTOR and eIF4E. After 72 hours, Western blotting with SCD1, mTOR, and eIF4E and actin was done. These results were confirmed in triplicate experiments. **B**, MDA-MB-468 cells were transfected with control siRNA or two separate sequences of eIF4E siRNA. After 72 hours, Western blotting with SCD1, eIF4E, and actin was done. **C**, MDA-MB-468 cells were transfected with single or pool siRNA for S6K1, and 72 hours later, Western blotting was done using S6K1, Akt, P-Akt (Thr 308), P-Akt (Ser 473), SCD1, SREBP1, eIF4E, and S6K1 was done (right). These results were confirmed in triplicate experiments. **D**, MCF7 cells were first transfected with siRNA for eIF4E. Dual luciferase assays were then done after cotransfecting with SCD1 promoter reporter (hSCD1-Luc pGL3) and control (pRL) plasmids. Treatment with and without rapamycin served as control. These results reflect an average of three independent experiments done in triplicate (left). MDA-MB-468, MCF7, and BT-474 cells were transfected with vector, 4E-BP1 WT, or 4E-BP1 5A plasmids. SCD1 promoter reporter (hSCD1-Luc pGL3) and control (pRL-TK) plasmids were cotransfected, and 96 hours later, dual luciferase assays were carried out. Vector transfection served as control. Analysis was done by using one-way ANOVA and Tukey post hoc test (right). This experiment was repeated three times in triplicate. Bars, SE.

To further confirm the role of PI3K/mTOR signaling in SCD1 expression, we studied the effects of LY294002, a dual PI3K and mTOR inhibitor (44). Similar to rapamycin, treatment with LY294002 led to the repression of SCD1 (Fig. 2D). In addition, we tested the effect of a new generation dual PI3K/mTOR inhibitor, BEZ235 (45). We found that BEZ235 treatment also led to a decrease in SCD1 levels, consistent with a role for PI3K/mTOR signaling in SCD1 expression (Fig. 2D).

Rapamycin regulates SCD1 promoter activity

To determine whether rapamycin affects the stability of SCD1 mRNA, MDA-MB-468 cells were cultured in either rapamycin or vehicle in the presence of 5 μ g/mL actinomycin D. The lack of a difference between the 24-hour trends of SCD1 mRNA levels in the two groups suggests that rapamycin does not affect SCD1 mRNA stability (Fig. 3A). We thus hypothesized that rapamycin regulates SCD1 transcription by inhibiting SCD1 promoter activity. We cultured MCF7 cells with rapamycin in the absence or presence of mevinolin, a known inducer of SCD1 promoter activity (21, 46). Western blot analysis showed that rapamycin repressed the induction of SCD1 protein expression by mevinolin (Fig. 3B). We next did a dual promoter assay (25). After cotransfecting MCF7 cells with SCD1 promoter reporter plasmid hSCD1-Luc pGL3 and control plasmid pRL-TK in triplicate, SCD1 promoter activity was significantly suppressed in the presence of rapamycin, both with and without mevinolin ($P = 0.013$ and $P = 0.009$, respectively; Fig. 3C). These results support the notion that rapamycin modulates SCD1 transcription by inhibiting SCD1 promoter activity.

Rapamycin regulates SREBP1

We next sought to determine how rapamycin suppresses SCD1 promoter activity. We focused on the SREBP1 transcription factor based on a recently proposed association between the PI3K/mTOR pathway and SREBP1 (47, 48). Both MDA-MB-468 and MCF7 cells exposed to rapamycin for 24 and 96 hours showed a decline in the mature active form of SREBP1 on Western blot (Fig. 4A). In addition, levels of SREBP1 precursor protein decreased in MCF7 at both time points. Once in the nucleus, the mature form of SREBP1 binds specifically to the SREBP response element (SRE) on the SCD1 promoter (25). The enzyme-linked immunosorbent assay (ELISA) was used to detect specific transcription factor DNA binding activity. The assay kit has a double-stranded DNA sequence containing the SRE immobilized onto wells of a 96-well plate. Nuclear extracts from both MCF7 and MDA-MB-468 cells treated with rapamycin for 24 and 96 hours showed a clear decrease in specific transcription factor DNA binding activity in the presence of rapamycin. The tabulated P values for both MCF7 ($P = 3.1 \times 10^{-10}$, $P = 0.00014$; Fig. 4B) and MDA-MB-468 ($P = 0.0014$, $P = 0.00054$; Fig. 4C) show this finding to be supportive of a role for rapamycin-mediated decrease in SREBP1 DNA binding activity. Be-

cause SREBP1 is known to regulate transcription of multiple genes in the fatty acid synthesis pathway, we studied the effects of rapamycin on two additional transcription targets (21). MDA-MB-468 cells treated with rapamycin for 96 hours also showed a suppression of ACC and FAS protein expression in addition to that of SCD1, suggesting a broader effect on fatty acid synthesis (Fig. 4D).

eIF4E plays a role in the regulation of both SCD1 and SREBP1

Activation of mTOR results in the phosphorylation of its effectors, the best studied of which are 4E-BP and S6K1 (49). Because rapamycin decreases 4E-BP1 phosphorylation (50), thereby decreasing the availability of eIF4E, we assessed the effect of eIF4E siRNA on SCD1 expression in MDA-MB-468 cells. We used the knockdown of mTOR by siRNA as a positive control. We found that mTOR knockdown decreased SCD1, consistent with our expectation that the effect of rapamycin on SCD1 occurs through decreased mTOR signaling. We found that eIF4E knockdown, like mTOR knockdown, also led to a decline in SCD1, suggesting a potential role for the mTOR/4E-BP1 axis in SCD1 regulation (Fig. 5A). We confirmed that two separate eIF4E siRNA sequences led to a decline in SCD1 levels (Fig. 5B). In MDA-MB-468 cells, silencing S6K1, an mTOR downstream target, neither reduced SCD1 levels nor increased P-Akt levels (Fig. 5C).

We then further studied the role of mTOR effectors on SREBP1. MDA-MB-468 cells were transfected with siRNA for eIF4E and S6K1. Western blot analysis showed a decrease in both precursor and mature forms of SREBP1 protein expression, as well as SCD1 expression for the eIF4E siRNA-transfected cells only (Fig. 5C). We next did a dual promoter assay using MCF7 cells cotransfected with SCD1 promoter reporter plasmid hSCD1-Luc pGL3 and control plasmid pRL-TK in triplicate; we found SCD1 promoter activity to be significantly suppressed with knockdown of eIF4E by siRNA. The level of relative promoter activity decline with eIF4E siRNA was similar to that observed with rapamycin ($P = 0.005$ and $P = 0.019$, respectively; Fig. 5D). Taken together, these results show a role for eIF4E in the regulation of SCD1.

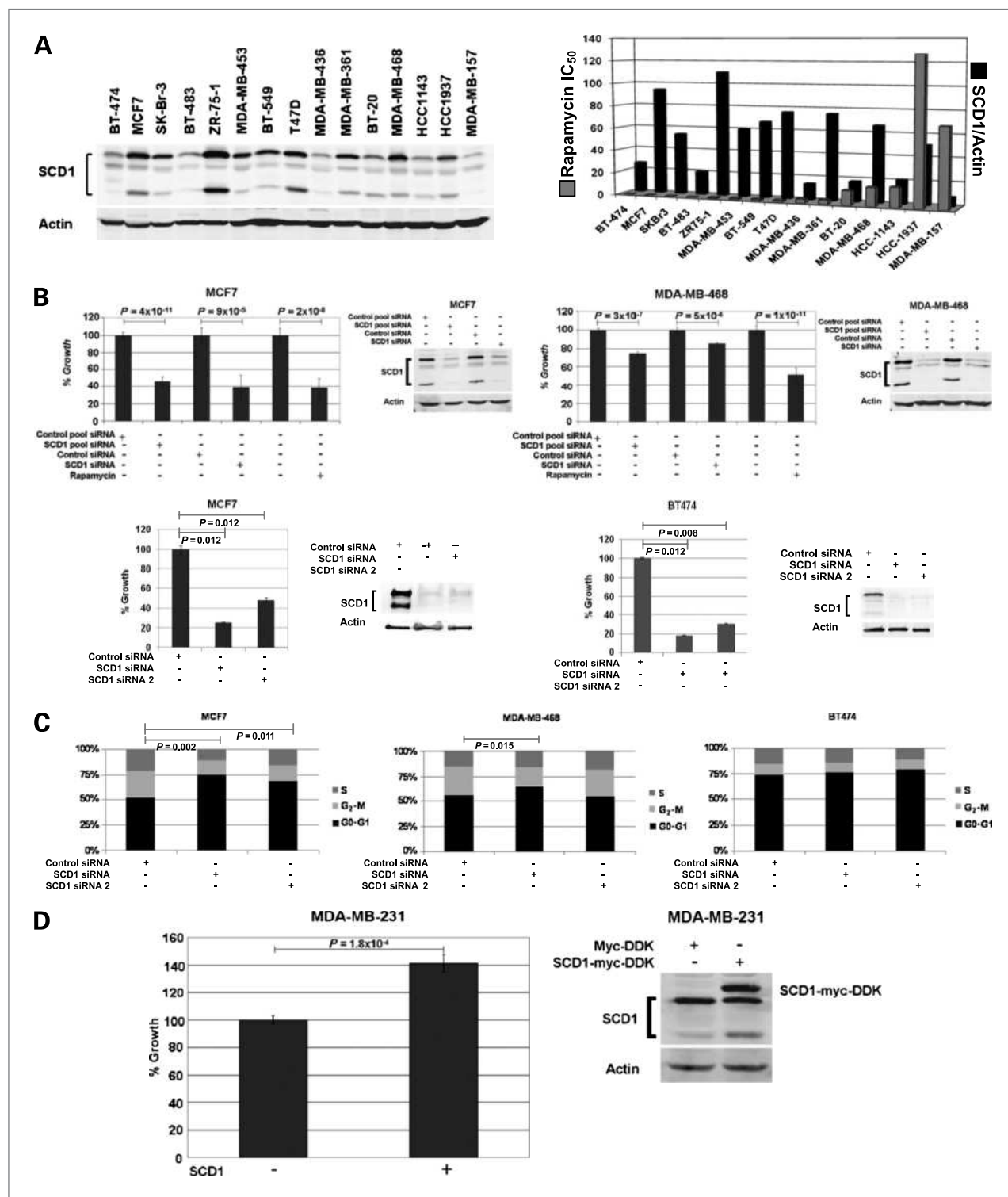
To support the role of 4E-BP1/eIF4E on expression of SCD1, we cotransfected SCD1 promoter reporter plasmid hSCD1-Luc pGL3 and control plasmid pRL-TK with empty vector or 4E-BP1 WT plasmid or 4E-BP1 5A plasmid using MDA-MB-468, BT-474, and MCF7 cell lines (Fig. 5D). Using dual promoter assay, we found SCD1 promoter activity to be significantly reduced with transfection of 4E-BP1 5A plasmid compared with empty vector and wild-type in all cell lines ($P < 0.05$).

SCD1 suppression and overexpression modulates cell growth

As SCD1 expression is regulated by mTOR signaling, we hypothesized that baseline SCD1 expression

itself may be a predictor of rapamycin sensitivity. To test this hypothesis, we quantified the baseline expression of SCD1 protein in a panel of 15 breast cancer cell lines by Western blotting (Fig. 6A). This panel of

cell lines was also treated with increasing concentrations of rapamycin and 5 days after exposure, growth inhibition was measured by SRB assay. Correlation between SCD1 expression and IC_{50} was not significant



(Spearman $r = -0.3424$, $P = 0.2116$; Fig. 6A). Thus, baseline level of SCD1 protein expression did not determine sensitivity of breast cancer cells to the growth-inhibitory action of rapamycin.

As mTOR is known to regulate cell growth, we sought to determine whether the suppression of SCD1 expression has any effect on cell growth. MCF7 and MDA-MB-468 cells were transfected with both single and pool SCD1 siRNA and their respective controls (Fig. 6B). One day after transfection, the cells were transferred to 96-well plates in quadruplicates. Treatment with rapamycin, a known suppressor of growth in both cell lines, was used as control (2). A parallel plate was maintained for subsequent Western blot analysis (Fig. 6B). Cell proliferation was assessed after 3 more days of culture by SRB assay. In both MCF7 cells and MDA-MB-468 cells, SCD1 pool and single siRNA knockdown led to a significant decrease in growth; Western blot analysis confirmed SCD1 knockdown. Statistically significant growth inhibition was obtained with SCD1 knockdown using two separate siRNA sequences in MCF7 and BT474 cells (Fig. 6B). SCD1 knockdown in MCF7 cells induced cell cycle arrest, as shown by a statistically significant increase in percentage of cells in G_0 - G_1 phase (50% G_0 - G_1 with control siRNA versus 70% with SCD1 siRNA, $P = 0.002$, and 61% with SCD1 siRNA 2, $P = 0.011$; Fig. 6C). SCD1 downregulation did not significantly affect cell cycle in MDA-MB-468 and BT474 cells. Taken together, however, these results show that suppression of SCD1 yields a significant decline in cell growth.

We next determined whether overexpression of SCD1 can increase cell growth. We used MDA-MB-231, a cell line with relative low expression of SCD1, to develop a stable SCD1-overexpressing cell line along with its respective control. Both overexpresser and control MDA-MB-231 were grown in 96-well plates. After 96 hours, an assay for cell number was done, yielding a significant increase in proliferation with the overexpression of SCD1 ($P = 1.8 \times 10^{-4}$; Fig. 6D). Western blot analysis confirmed the presence of exogenous SCD1 expression (Fig. 6D).

Discussion

Rapamycin and its analogs are currently undergoing extensive study to evaluate the determinants of their antitumor efficacy. Identifying how rapamycin affects the high rate of metabolism required for tumor growth is an important first step that could lead to useful biomarkers or effective rational combinatorial therapy. The role of mTOR in cellular metabolism is emphasized by its ability to control amino acid biosynthesis, glucose homeostasis, and adipogenesis (17). We show that mTOR signaling regulates SCD1 expression. We propose that the link between mTOR and SCD1 is one of the key interactions that may play a role in the effect of mTOR on tumor growth and metabolism.

mTOR is a critical regulator of protein translation. Rapamycin inhibits mTOR complex 1 signaling, resulting in dephosphorylation of its effectors, the best studied of which are 4E-BP1 and S6K1. Hyperphosphorylation of 4E-BP1 leads to inhibition of binding of 4E-BP to eIF4E, which decreases the amount of eIF4E available to initiate cap-dependent translation. S6K1 phosphorylates ribosomal protein S6, in some models enhancing the translation of mRNAs possessing a 5' terminal oligopyrimidine tract (51). S6K1 phosphorylates several other translational regulators, including eukaryotic initiation factor 4B, programmed cell death 4, and eukaryotic elongation factor-2 kinase (52). Although we initially identified SCD1 as a mRNA that is decreased in polysomes upon rapamycin treatment in all three cell lines, we found that this is primarily a reflection of a drop in total SCD1 mRNA levels due to inhibition of SCD1 promoter activity, rather than due to a significant inhibition of polysomal recruitment. Induction of SCD1 expression or promoter activity by insulin and abolishment of this activity by rapamycin was shown in liver cancer (47), but the players connecting mTOR and SCD1 are not very well defined. S6K1 activates liver X receptor α (LXR α), and LXR α promotes lipogenesis by regulating expression of lipogenic genes, including *SREBP1* (53). We could not show involvement of S6K1 in regulation of SCD1 expression; interestingly, however, we found that silencing eIF4E also resulted in

Figure 6. SCD1 regulates breast cancer cell growth. A, left, baseline SCD1 protein expression in 15 breast cancer cell lines. Western blotting was done using SCD1 and actin antibody. Right, SCD1 and actin bands were quantified; the average of three independent experiments is shown as relative SCD1/actin expression. The same chart shows IC_{50} values of breast cancer cell lines. Cells were treated with increasing concentrations of rapamycin for 5 days and IC_{50} was determined on the basis of the dose-response curves using SRB assay. B, MCF7 cells (top left) and MDA-MB-468 cells (top right) were transfected with single or pool control siRNA and SCD1 siRNA. Cells were grown in medium supplemented with lipid-deficient serum and cell growth analysis was then done with readings recorded after 96 hours of treatment by SRB assay. Cells treated with and without rapamycin were the designated controls. These results reflect experiments done in triplicate. Western blotting with SCD1 and actin were done on the treated cells of both MCF7 and MDA-MB-468 cells to confirm adequate suppression of SCD1 by siRNA after 96 hours. MCF7 cells (bottom left) and BT474 cells (bottom right) were transfected with single control siRNA, SCD1 siRNA, or a SCD1 siRNA 2. Cells were grown in regular medium and cell growth analysis was then done with readings recorded after 96 hours of treatment by SRB assay. SCD1 siRNA-treated cells were compared with control siRNA-treated cells using Student's *t*-test. These results are representative of two independent experiments. C, MCF7 (left), MDA-MB-468 (middle), and BT474 cells (right) were transfected with single control siRNA, SCD1 siRNA, or a SCD1 siRNA 2. Cells were grown in regular medium and analyzed for cell cycle profile after 96 hours. Percentage of cells in G_0 - G_1 was compared using Student's *t*-test. D, MDA-MB-231 SCD1 overexpressing stable cells were grown alongside control in media supplemented with lipid-deficient serum. Cell growth analysis was then done with readings recorded after 96 hours of growth. These results reflect experiments done in triplicate (left). Western blotting with SCD1 and actin was done on MDA-MB-231-overexpressing stable cells alongside their respective control to confirm expression of the transfected myc-tagged SCD1 protein (right).

the inhibition of SCD1 promoter activity and subsequent expression, suggesting that SCD1 is downstream of eIF4E. Further work is needed to determine whether the effect of rapamycin on SCD1 is mediated through the regulation of SREBP1 expression by eIF4E. Indeed, our results show that both precursor and mature forms of SREBP1 are affected in the presence of eIF4E suppression. Additionally, although eIF4E is a principal modulator of translation initiation (54), recent studies have shown that it maintains a presence in the nucleus and may play a role in both selective mRNA export and post-transcriptional modulation (55, 56). This suggests the presence of a signaling module from mTOR to eIF4E to SREBP1 culminating in SCD1. The module is likely to regulate a suite of enzymes involved in fatty acid synthesis due to the activity of SREBP1 in coordinate promoter regulation of this group of enzymes.

Obesity in postmenopausal women is a risk factor for developing breast cancer (57). Hormones (estrogen) and adipokines such as leptin and IGF-I all show mitogenic effects in MCF7 cells and stimulate cell proliferation in mammary glands of obese rats, suggesting an increase in risk for breast cancer (58). The role that human SCD1 plays in the production of monounsaturated fatty acids makes it an important factor in cellular fat metabolism and a novel target in the prevention of obesity-associated breast cancer. Studies in mice point to a clear downregulation of the genes involved in lipogenesis when SCD1 expression is decreased (59). These studies show that SCD1 plays a central role in cellular fat metabolism, further highlighting the significance of our current findings. SCD1 is already being pursued as a therapeutic target for obesity (60, 61). Recent data suggest that SCD1 may also hold promise as a cancer therapy target (16). To better define the role of SCD1 in breast cancer biology, we sought to determine the effects of both knockdown and overexpression of SCD1 on breast cancer cell growth *in vitro*. Transient knockdown of SCD1 yields a significant drop in cell growth/proliferation, whereas overexpression yields elevated cell proliferation. These findings support the notion that SCD1

is a novel mediator of breast cancer cell growth and further supports the case that SCD1 is indeed a promising cancer therapy target.

In summary, we have established the mTOR signaling pathway as a major regulator of SCD1 expression in breast cancer cells. This highlights a previously underappreciated link between oncogenic cell signaling and cancer cell fat metabolism. We have also begun to define the role of SCD1 in breast cancer. Studies are ongoing to assess the potential of SCD1 as a marker of activity of mTOR signaling, as well as potential pharmacodynamic marker of response to mTOR inhibitors. Further studies are needed to evaluate the role of SCD1 in the breast cancer malignant phenotype, and ultimately to determine the role of SCD1 as a therapeutic target either alone or in combination with rapamycin.

Disclosure of Potential Conflicts of Interest

F. Meric-Bernstam: clinical trial support Novartis Pharma and Abraxis; honorarium Novartis Pharma. A.M. Gonzalez-Angulo: clinical trial support Novartis Pharma and Abraxis.

Acknowledgments

We thank Judy Roehm for assistance with manuscript preparation and Dr. James M. Ntambi for the gift of the SCD1 promoter reporter plasmid hSCD1-Luc pGL3, Dr. Philip N. Tsichlis for the gift of the constitutively active Akt plasmid, and Dr. Thurl E. Harris for the gift of the 4E-BP1 mutant plasmids.

Grant Support

NIH1 R01 CA112199 (F. Meric-Bernstam), Elsa Pardee Foundation (F. Meric-Bernstam), Society of Surgical Oncology Clinical Investigator Award (F. Meric-Bernstam), National Center for Research Resources grant 1UL1RR024148 (F. Meric-Bernstam and L. Zhang), NIH 5 T32 CA09599 (F. Meric-Bernstam, D. Luyimbazi, and P.F. McAuliffe), Kleberg Center for Molecular Markers (F. Meric-Bernstam, A.M. Gonzalez-Angulo, G.B. Mills) and the U. T. M. D. Anderson Cancer Center Support Core Grant (CA 16672).

The costs of publication of this article were defrayed in part by the payment of page charges. This article must therefore be hereby marked *advertisement* in accordance with 18 U.S.C. Section 1734 solely to indicate this fact.

Received 10/30/2009; revised 08/11/2010; accepted 08/11/2010; published OnlineFirst 09/28/2010.

References

- Hidalgo M, Rowinsky EK. The rapamycin-sensitive signal transduction pathway as a target for cancer therapy. *Oncogene* 2000;19:6680–6.
- Noh WC, Mondesire WH, Peng J, et al. Determinants of rapamycin sensitivity in breast cancer cells. *Clin Cancer Res* 2004;10:1013–23.
- Mondesire WH, Jian W, Zhang H, et al. Targeting mammalian target of rapamycin synergistically enhances chemotherapy-induced cytotoxicity in breast cancer cells. *Clin Cancer Res* 2004;10:7031–42.
- Yu K, Toral-Barza L, Discafani C, et al. mTOR, a novel target in breast cancer: the effect of CCI-779, an mTOR inhibitor, in preclinical models of breast cancer. *Endocr Relat Cancer* 2001;8:249–58.
- Meric-Bernstam F, Esteva FJ. Potential role of mammalian target of rapamycin inhibitors in breast cancer therapy. *Clin Breast Cancer* 2005;6:357–60.
- Chan S, Scheulen ME, Johnston S, et al. Phase II study of temsirolimus (CCI-779), a novel inhibitor of mTOR, in heavily pretreated patients with locally advanced or metastatic breast cancer. *J Clin Oncol* 2005;23:5314–22.
- Ellard SL, Clemons M, Gelmon KA, et al. Randomized phase II study comparing two schedules of everolimus in patients with recurrent/metastatic breast cancer: NCIC Clinical Trials Group IND.163. *J Clin Oncol* 2009;27:4536–41.
- Enoch HG, Catala A, Strittmatter P. Mechanism of rat liver microsomal stearyl-CoA desaturase. Studies of the substrate specificity, enzyme-substrate interactions, and the function of lipid. *J Biol Chem* 1976;251:5095–103.

9. Ntambi JM. Regulation of stearyl-CoA desaturase by polyunsaturated fatty acids and cholesterol. *J Lipid Res* 1999;40:1549–58.
10. Ntambi JM. The regulation of stearyl-CoA desaturase (SCD). *Prog Lipid Res* 1995;34:139–50.
11. Liu S, Umez-Goto M, Murph M, et al. Expression of autotaxin and lysophosphatidic acid receptors increases mammary tumorigenesis, invasion, and metastases. *Cancer Cell* 2009;15:539–50.
12. Li J, Ding SF, Habib NA, Fermor BF, Wood CB, Gilmour RS. Partial characterization of a cDNA for human stearyl-CoA desaturase and changes in its mRNA expression in some normal and malignant tissues. *Int J Cancer* 1994;57:348–52.
13. Habib NA, Wood CB, Apostolov K, et al. Stearic acid and carcinogenesis. *Br J Cancer* 1987;56:455–8.
14. Falvella FS, Pascale RM, Gariboldi M, et al. Stearyl-CoA desaturase 1 (Scd1) gene overexpression is associated with genetic predisposition to hepatocarcinogenesis in mice and rats. *Carcinogenesis* 2002;23:1933–6.
15. Pascale RM, Simile MM, DeMiglio MR, et al. The BN rat strain carries dominant hepatocarcinogen resistance loci. *Carcinogenesis* 1996;17:1765–8.
16. Morgan-Lappe SE, Tucker LA, Huang X, et al. Identification of Ras-related nuclear protein, targeting protein for xenopus kinesin-like protein 2, and stearyl-CoA desaturase 1 as promising cancer targets from an RNAi-based screen. *Cancer Res* 2007;67:4390–8.
17. Wullschlegel S, Loewith R, Hall MN. TOR signaling in growth and metabolism. *Cell* 2006;124:471–84.
18. El-Chaar D, Gagnon A, Sorisky A. Inhibition of insulin signaling and adipogenesis by rapamycin: effect on phosphorylation of p70 S6 kinase vs eIF4E-BP1. *Int J Obes Relat Metab Disord* 2004;28:191–8.
19. Yu W, Chen Z, Zhang J, et al. Critical role of phosphoinositide 3-kinase cascade in adipogenesis of human mesenchymal stem cells. *Mol Cell Biochem* 2008;310:11–8.
20. Zhang HH, Huang J, Duvel K, et al. Insulin stimulates adipogenesis through the Akt-TSC2–1 pathway. *PLoS One* 2009;4:e6189.
21. Brown MS, Goldstein JL. The SREBP pathway: regulation of cholesterol metabolism by proteolysis of a membrane-bound transcription factor. *Cell* 1997;89:331–40.
22. Choi JH, Bertram PG, Drenan R, Carvalho J, Zhou HH, Zheng XF. The FKBP12-rapamycin-associated protein (FRAP) is a CLIP-170 kinase. *EMBO Rep* 2002;3:988–94.
23. Vlahos CJ, Matter WF, Hui KY, Brown RF. A specific inhibitor of phosphatidylinositol 3-kinase, 2-(4-morpholinyl)-8-phenyl-4H-1-benzopyran-4-one (LY294002). *J Biol Chem* 1994;269:5241–8.
24. Maira SM, Stauffer F, Brueggen J, et al. Identification and characterization of NVP-BE235, a new orally available dual phosphatidylinositol 3-kinase/mammalian target of rapamycin inhibitor with potent *in vivo* antitumor activity. *Mol Cancer Ther* 2008;7:1851–63.
25. Bene H, Lasky D, Ntambi JM. Cloning and characterization of the human stearyl-CoA desaturase gene promoter: transcriptional activation by sterol regulatory element binding protein and repression by polyunsaturated fatty acids and cholesterol. *Biochem Biophys Res Commun* 2001;284:1194–8.
26. Soni A, Akcakanat A, Singh G, et al. eIF4E knockdown decreases breast cancer cell growth without activating Akt signaling. *Mol Cancer Ther* 2008;7:1782–8.
27. Kim DH, Sarbassov DD, Ali SM, et al. mTOR interacts with raptor to form a nutrient-sensitive complex that signals to the cell growth machinery. *Cell* 2002;110:163–75.
28. Lynch M, Chen L, Ravitz MJ, et al. hnRNP K binds a core polypyrimidine element in the eukaryotic translation initiation factor 4E (eIF4E) promoter, and its regulation of eIF4E contributes to neoplastic transformation. *Mol Cell Biol* 2005;25:6436–53.
29. Kim D, Akcakanat A, Singh G, Sharma C, Meric-Bernstam F. Regulation and localization of ribosomal protein S6 kinase 1 isoforms. *Growth Factors* 2009;27:12–21.
30. Hennessy BT, Gilcrease MZ, Kim E, Gonzalez-Angulo AM. Breast carcinoma with neuroendocrine differentiation and myocardial metastases. *Clin Breast Cancer* 2007;7:892–4.
31. Moreno A, Akcakanat A, Munsell MF, Soni A, Yao JC, Meric-Bernstam F. Antitumor activity of rapamycin and octreotide as single agents or in combination in neuroendocrine tumors. *Endocr Relat Cancer* 2008;15:257–66.
32. Akcakanat A, Zhang L, Tsavachidis S, Meric-Bernstam F. The rapamycin-regulated gene expression signature determines prognosis for breast cancer. *Mol Cancer* 2009;8:75.
33. Dong J, Peng J, Zhang H, et al. Role of glycogen synthase kinase 3beta in rapamycin-mediated cell cycle regulation and chemosensitivity. *Cancer Res* 2005;65:1961–72.
34. Zhang L, Miles MF, Aldape KD. A model of molecular interactions on short oligonucleotide microarrays. *Nat Biotechnol* 2003;21:818–21.
35. Pounds S, Morris SW. Estimating the occurrence of false positives and false negatives in microarray studies by approximating and partitioning the empirical distribution of *P*-values. *Bioinformatics* 2003;19:1236–42.
36. Gera JF, Mellinckhoff IK, Shi Y, et al. AKT activity determines sensitivity to mammalian target of rapamycin (mTOR) inhibitors by regulating cyclin D1 and c-myc expression. *J Biol Chem* 2004;279:2737–46.
37. Rajasekhar VK, Viale A, Socci ND, Wiedmann M, Hu X, Holland EC. Oncogenic Ras and Akt signaling contribute to glioblastoma formation by differential recruitment of existing mRNAs to polysomes. *Mol Cell* 2003;12:889–901.
38. Raymond E, Alexandre J, Faivre S, et al. Safety and pharmacokinetics of escalated doses of weekly intravenous infusion of CCI-779, a novel mTOR inhibitor, in patients with cancer. *J Clin Oncol* 2004;22:2336–47.
39. Hidalgo M, Buckner JC, Erlichman C, et al. A phase I and pharmacokinetic study of temsirolimus (CCI-779) administered intravenously daily for 5 days every 2 weeks to patients with advanced cancer. *Clin Cancer Res* 2006;12:5755–63.
40. Zhang L, Ge L, Parimoo S, Stenn K, Prouty SM. Human stearyl-CoA desaturase: alternative transcripts generated from a single gene by usage of tandem polyadenylation sites. *Biochem J* 1999;340:255–64.
41. Heinemann FS, Ozols J. Degradation of stearyl-coenzyme A desaturase: endoproteolytic cleavage by an integral membrane protease. *Mol Biol Cell* 1998;9:3445–53.
42. Brunn GJ, Hudson CC, Sekulic A, et al. Phosphorylation of the transcriptional repressor PHAS-I by the mammalian target of rapamycin. *Science* 1997;277:99–101.
43. von Manteuffel SR, Dennis PB, Pullen N, Gingras AC, Sonenberg N, Thomas G. The insulin-induced signalling pathway leading to S6 and initiation factor 4E binding protein 1 phosphorylation bifurcates at a rapamycin-sensitive point immediately upstream of p70s6k. *Mol Cell Biol* 1997;17:5426–36.
44. Brunn GJ, Williams J, Sabers C, Wiederrecht G, Lawrence JC, Jr., Abraham RT. Direct inhibition of the signaling functions of the mammalian target of rapamycin by the phosphoinositide 3-kinase inhibitors, wortmannin and LY294002. *EMBO J* 1996;15:5256–67.
45. Serra V, Markman B, Scaltriti M, et al. NVP-BE235, a dual PI3K/mTOR inhibitor, prevents PI3K signaling and inhibits the growth of cancer cells with activating PI3K mutations. *Cancer Res* 2008;68:8022–30.
46. Tabor DE, Kim JB, Spiegelman BM, Edwards PA. Identification of conserved cis-elements and transcription factors required for sterol-regulated transcription of stearyl-CoA desaturase 1 and 2. *J Biol Chem* 1999;274:20603–10.
47. Mauvoisin D, Rocque G, Arfa O, Radenne A, Boissier P, Mounier C. Role of the PI3-kinase/mTOR pathway in the regulation of the stearyl CoA desaturase (SCD1) gene expression by insulin in liver. *J Cell Commun Signal* 2007;1:113–25.
48. Porstmann T, Santos CR, Griffiths B, et al. SREBP activity is regulated by mTORC1 and contributes to Akt-dependent cell growth. *Cell Metab* 2008;8:224–36.
49. Meric-Bernstam F, Gonzalez-Angulo AM. Targeting the mTOR signaling network for cancer therapy. *J Clin Oncol* 2009;27:2278–87.
50. Gingras AC, Kennedy SG, O'Leary MA, Sonenberg N, Hay N. 4E-BP1, a repressor of mRNA translation, is phosphorylated and inactivated by the Akt(PKB) signaling pathway. *Genes Dev* 1998;12:502–13.
51. Jefferies HB, Fumagalli S, Dennis PB, Reinhard C, Pearson RB,

- Thomas G. Rapamycin suppresses 5'TOP mRNA translation through inhibition of p70s6k. *EMBO J* 1997;16:3693–704.
52. Jastrzebski K, Hannan KM, Tchoubrieva EB, Hannan RD, Pearson RB. Coordinate regulation of ribosome biogenesis and function by the ribosomal protein S6 kinase, a key mediator of mTOR function. *Growth Factors* 2007;25:209–26.
 53. Hwahng SH, Ki SH, Bae EJ, Kim HE, Kim SG. Role of adenosine monophosphate-activated protein kinase-p70 ribosomal S6 kinase-1 pathway in repression of liver X receptor-alpha-dependent lipogenic gene induction and hepatic steatosis by a novel class of dithiolethiones. *Hepatology* 2009;49:1913–25.
 54. Meric F, Hunt KK. Translation initiation in cancer: a novel target for therapy. *Mol Cancer Ther* 2002;1:971–9.
 55. Andrei MA, Ingelfinger D, Heintzmann R, Achsel T, Rivera-Pomar R, Luhrmann R. A role for eIF4E and eIF4E-transporter in targeting mRNPs to mammalian processing bodies. *RNA* 2005;11:717–27.
 56. Strudwick S, Borden KL. The emerging roles of translation factor eIF4E in the nucleus. *Differentiation* 2002;70:10–22.
 57. Cleary MP, Grossmann ME. Minireview: obesity and breast cancer: the estrogen connection. *Endocrinology* 2009;150:2537–42.
 58. Lautenbach A, Budde A, Wrann CD, et al. Obesity and the associated mediators leptin, estrogen and IGF-I enhance the cell proliferation and early tumorigenesis of breast cancer cells. *Nutr Cancer* 2009;61:484–91.
 59. Ntambi JM, Miyazaki M, Stoehr JP, et al. Loss of stearoyl-CoA desaturase-1 function protects mice against adiposity. *Proc Natl Acad Sci U S A* 2002;99:11482–6.
 60. Dobrzyn A, Ntambi JM. Stearoyl-CoA desaturase as a new drug target for obesity treatment. *Obes Rev* 2005;6:169–74.
 61. Liu G, Lynch JK, Freeman J, et al. Discovery of potent, selective, orally bioavailable stearoyl-CoA desaturase 1 inhibitors. *J Med Chem* 2007;50:3086–100.